Alkaline volcanic rocks from the Columbia Hills, Gusev crater, Mars

H. Y. McSween,[1] S. W. Ruff,[2] R. V. Morris,[3] J. F. Bell III,[4] K. Herkenhoff,[5] R. Gellert,[6] K. R. Stockstill,[7] L. L. Tornabene,[1] S. W. Squyres,[4] J. A. Crisp,[8] P. R. Christensen,[2] T. J. McCoy,[9] D. W. Mittlefehldt,[3] and M. Schmidt[9]

[1] Irvine, Backstay, and Wishstone are the type specimens for three classes of fine-grained or fragmental, relatively unaltered rocks with distinctive thermal emission spectra, found as float on the flanks of the Columbia Hills. Chemical analyses indicate that these rocks are mildly alkaline basalt, trachybasalt, and tephrite, respectively. Their mineralogy consists of Na- and K-rich feldspar(s), low- and high-Ca pyroxenes, ferroan olivine, Fe-Ti (and possibly Cr) oxides, phosphate, and possibly glass. The texture of Wishstone is consistent with a pyroclastic origin, whereas Irvine and Backstay are lavas or possibly dike rocks. Chemical compositions of these rocks plot on or near liquid lines of descent for most elements calculated for Adirondack class rocks (olivine-rich basalts from the Gusev plains) at various pressures from 0.1 to 1.0 GPa. We infer that Wishstone-, Backstay-, and Irvine-class magmas may have formed by fractionation of primitive, oxidized basaltic magma similar to Adirondack-class rocks. The compositions of all these rocks reveal that the Gusev magmatic province is alkaline, distinct from the subalkaline volcanic rocks thought to dominate most of the planet's surface. The fact that differentiated volcanic rocks were not encountered on the plains prior to ascending Husband Hill may suggest a local magma source for volcanism beneath Gusev crater.

1. Introduction

[2] Terrestrial magmatic rocks are classified as subalkaline or alkaline, distinguished by comparing the molar concentrations of alkalis and silica. The Spirit rover measured high $Na_2O + K_2O$ and low SiO_2 abundances in picritic (olivine-rich) basalts, termed Adirondack-class rocks [*Squyres et al.*, 2006], on the plains of Gusev crater [*Gellert et al.*, 2004; *McSween et al.*, 2004, 2006]. The compositions of these rocks straddle the boundary between the subalkaline and alkaline fields. Once Spirit began

climbing into the Columbia Hills at West Spur, it encountered outcrops of altered rocks and attention shifted to these materials [*Arvidson et al.*, 2006]. During the ascent of Husband Hill, the rover found numerous, minimally weathered float rocks, defined as the Wishstone class [*Squyres et al.*, 2006]. Midway up the northwest flank, a few isolated float rocks (dark, apparently unaltered, and clearly distinct from the outcrops and other float samples) were observed and defined as the Backstay class [*Squyres et al.*, 2006]. At the crest of Husband Hill another type of dark rock was distinguished, which we here call the Irvine class. All three classes were initially recognized on the basis of their distinctive MiniTES (Miniature Thermal Emission Spectrometer) spectra [*Ruff et al.*, 2006]. The type specimens for these classes (Wishstone, Backstay, and Irvine) have been characterized using the full Athena instrument payload, which also includes visible/near-infrared spectral (Panoramic Camera, Pancam), textural (Microscopic Imager, MI), chemical (Alpha Particle X-ray Spectrometer, APXS), and mineralogical (Mössbauer Spectrometer, MB) measurements. Here we describe these rocks, which have alkaline compositions. We also explore their possible petrogenetic relationship to Adirondack-class basalts on the Gusev plains.

[3] These rocks, interpreted as volcanic or volcaniclastic samples, are the first alkaline rocks recognized on Mars. The Martian surface is thought to be dominated by subalkaline rocks, on the basis of rock compositions inferred from

[1]Department of Earth and Planetary Sciences, University of Tennessee, Knoxville, Tennessee, USA.

[2]Department of Geological Sciences, Arizona State University, Tempe, Arizona, USA.

[3]NASA Johnson Space Center, Houston, Texas, USA.

[4]Department of Astronomy, Cornell University, Ithaca, New York, USA.

[5]Astrogeology Branch, U.S. Geological Survey, Flagstaff, Arizona, USA.

[6]Department of Physics, University of Guelph, Guelph, Canada.

[7]Hawaii Institute of Geophysics and Planetology, University of Hawaii at Manoa, Honolulu, Hawaii, USA.

[8]Jet Propulsion Laboratory, California Institute of Technology, Pasadena, California, USA.

[9]Department of Mineral Sciences, Smithsonian Institution, Washington, D. C., USA.

orbital spectroscopy [*Mustard et al.*, 1993; *Bandfield et al.*, 2000; *Hamilton et al.*, 2001] and the analyzed compositions of basaltic Martian (SNC) meteorites [*McSween*, 2002]. In hindsight, however, the discovery of alkaline rocks somewhere on Mars should have been predictable. Geochemical models for the Martian mantle have higher contents of volatile elements, including the alkalis, than in the Earth's mantle [*Dreibus and Wänke*, 1985; *Lodders and Fegley*, 1997; *Sanloup et al.*, 1999], and partial melting of such mantle compositions at high pressures could yield alkalic magmas.

2.   Analytical Methods

[4] Descriptions of the acquisition and calibration of Pancam spectra were given by *Bell et al.* [2003, 2006], and of MiniTES spectra by *Christensen et al.* [2003] and *Ruff et al.* [2006]. Pancam spectra of Wishstone-class rocks [*Farrand et al.*, 2006] and MiniTES spectra of Wishstone- and Backstay-class rocks [*Ruff et al.*, 2006] were previously published, but Irvine spectra were not presented in those papers. Pancam spectra of Wishstone and Champagne, a similar member of the Wishstone class, were obtained for surfaces ground using the Rock Abrasion Tool (RAT). Wearing away of the Spirit RAT's diamond grinding teeth after more than 400 sols of operations prevented grinding of Backstay and Irvine (both encountered after sol 500) to expose their interiors. Most spectra for Backstay- and Irvine-class rocks are for natural rock surfaces; the one exception is Backstay itself, which was also brushed using the RAT. MiniTES spectra of the natural surfaces of Backstay and Irvine do not display any obvious spectral features of dust, suggesting that the surfaces of the spectrally examined rocks are relatively clean, but Pancam observations indicate that some dust covers parts of the natural rock surfaces. A dust coating on Spirit's MiniTES pointing mirror acquired on or about sol 420 complicates the deconvolution of later spectra [*Ruff et al.*, 2006], and all Backstay- and Irvine-class rocks were encountered after this dusting event. However, the MiniTES spectra for Wishstone and some other rocks of this class were obtained earlier, and an average Wishstone-class spectrum can be deconvolved without difficulty [*Ruff et al.*, 2006].

[5] MI images, acquired using procedures described by *Herkenhoff et al.* [2003], were taken of RAT-abraded (RATed) Wishstone and Champagne [*Herkenhoff et al.*, 2006], and of unbrushed Irvine and RAT-brushed Backstay. Acquisition of APXS data was described by *Rieder et al.* [2003] with revised calibrations by *Gellert et al.* [2006], and of MB data by *Klingelhöfer et al.* [2003]. The compilation of APXS data by *Gellert et al.* [2006] includes analyses of RATed Wishstone and Champagne, but the APXS data for Backstay and Irvine in this paper have not been previously published. The compositions of unbrushed and brushed Backstay are very similar, supporting the contention that this rock surface is relatively free of dust, although the brushed surface has less sulfur indicating some dust removal. MB data for RATed Wishstone and Champagne were tabulated and interpreted by *Morris et al.* [2006]. MB data for Backstay and Irvine were taken from brushed and unbrushed surfaces, respectively, and have not been previously published. *Morris et al.* [2006] indicated that all

nanophase oxides, hematite, and sulfates were alteration products and thus their sum could be used as an alteration index; using this scheme, Wishstone, Backstay, and Irvine are among the least altered rocks in the Columbia Hills.

3.   Field Occurrence and Geologic Context

[6] Wishstone-class rocks have only been identified as float, but they are widespread (at least 95 rocks of this class have been identified from MiniTES spectra) on the north-western flank of Husband Hill [*Arvidson et al.*, 2006; *Ruff et al.*, 2006]. Backstay was found near the crest of Cumberland Ridge, and other Backstay-class rocks were encountered only on the upper portions of Husband Hill, at elevations >50 m above the surrounding plains [*Squyres et al.*, 2006]. All Backstay-class rocks are also float. Irvine is one in a set of aligned rocks (Figure 1a) found on the summit plateau of Husband Hill, ~90 m above the plains. These aligned rocks all have similar MiniTES spectral properties and might represent the surface expression of a dike or sill, although imaging from several vantage points could not confirm that these rocks were outcrop rather than float. Two other rocks with Irvine-like spectra were observed well away from the alignment in nearly perpendicular directions (4.5 m to the south and 20 m to the north). These samples are the only Irvine-class rocks found. At least nine different rocks with Backstay spectral character and up to seven with Irvine spectral character have been observed on Husband Hill. No Wishstone-, Irvine-, or Backstay-class rocks were encountered on the plains prior to ascending the Columbia Hills, despite MiniTES spectral measurements of hundreds of rocks. Their restricted distribution may reflect eruption from a local magmatic source beneath Husband Hill or importation as impact ejecta derived from compositionally distinct units in another part of the crater (J. A. Grant et al., The distribution of rocks on the Gusev plains and on Husband Hill, manuscript in preparation, 2006; hereinafter referred to as Grant et al., manuscript in preparation, 2006).

[7] Wishstone (Figure 1b), like other members of its class, has a surface decorated with closely spaced knobs and pits. The knobs apparently represent small clasts that are resistant to eolian abrasion. The specific grinding energies for Wishstone and Champagne indicate that they are harder than outcrop rocks in the Hills [*Squyres et al.*, 2006]. Irvine (Figure 1a) and Backstay (Figure 1c) are smooth and faceted, presumably by eolian erosion. Both rocks also show small but less common pits, possibly eroded vesicles or soft minerals. Like other members of their classes, these rocks are dark and generally featureless. However, faint lineations are seen on the surface of Backstay, as well as some small knobs. No specific grinding energies are available for these rocks.

[8] Microscopic images of RAT-ground Wishstone (Figure 2a) and Champagne (Figure 2b) reveal angular clasts or grains of varying sizes. The textures of Wishstone-class rocks resemble pyroclastic tuffs [*Farrand et al.*, 2006; *Squyres et al.*, 2006], although an origin as impact ejecta cannot be ruled out [*Ming et al.*, 2006]. MI images of Irvine (Figure 2c) and Backstay (Figure 2d) show that both rocks are aphanitic, without the clasts seen in Wishstone-class rocks or the large dark crystals seen in Adirondack-class basalts
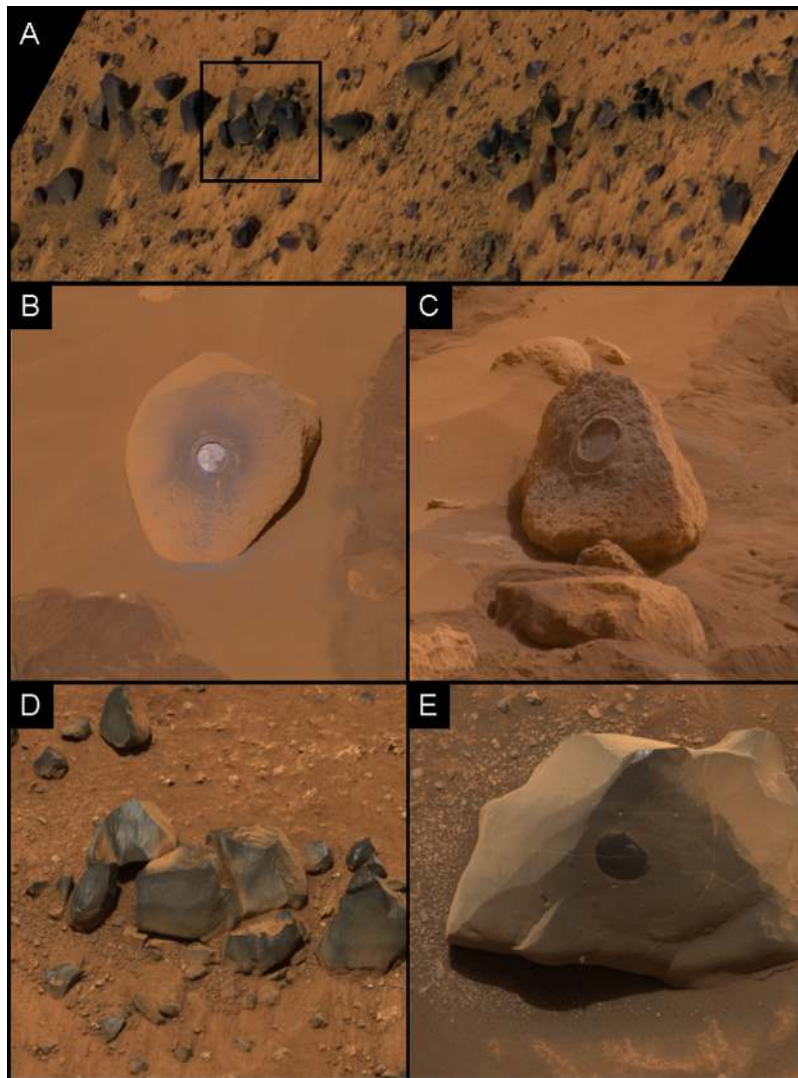
Figure 1. True-color Pancam images of analyzed rocks. (a) Aligned Irvine-class rocks (∼2 m long) at the summit of Husband Hill. The pattern may suggest that these rocks are samples of a dike. (b) Wishstone (rock is ∼27 cm across) after RAT grinding. (c) Champagne (rock is ∼18 cm across) after RAT grinding. (d) Irvine (image is 25 cm across). (e) Backstay (rock is 20 cm high) after the RAT had brushed the surface and revealed a darker interior.

[*McSween et al.*, 2004, 2006]. However, the lack of ground and polished (RATed) surfaces on these rocks may hamper the recognition of crystals in MI images. Backstay and Irvine are interpreted as rocks from volcanic flows or possibly dikes.

[9] Pancam, MiniTES, and MB spectra suggest that Wishstone-, Backstay-, and Irvine-class rocks are relatively unaltered and unweathered, unlike outcrops that comprise the Columbia Hills [*Farrand et al.*, 2006; *Ming et al.*, 2006; *Morris et al.*, 2006]. This conclusion is supported by their relatively low contents of sulfur and halides. Consequently, they are presumed to be younger than the Hills outcrops. No geologic relationships constrain their age relative to the unaltered Adirondack-class basalts on the plains, allowing the possibility that they might be correlative. Grant et al. (manuscript in preparation, 2006) suggest that the float rocks in the Hills (if they are ejecta) are older than the Adirondack-class basalts, because no examples of these three classes occur on the plains. They could be contemporaneous, however, if these classes intruded the Hills as dikes. The source of the plains basaltic flows is unknown, but they must be younger than the Columbia Hills onto which they lap [*Arvidson et al.*, 2006]. These flows might derive from the huge Apollinaris volcano north of Gusev or other, more proximal volcanic vents [*Martínez-Alonso et al.*, 2005; *McSween et al.*, 2006], although no flows have been traced from any of these possible sources into the crater. Wishstone-class rocks are plausibly tuffs derived from the eruption of Apollinaris, but may still have been excavated and lofted onto Husband Hill by an impact. It is very doubtful that any lava flows overtopped the Columbia Hills, given the small amounts of volcanic float present. More likely, the Backstay- and Irvine-class rocks were lofted onto the Hills as ejecta blocks or were intruded from below to form small dikes or sills. If the aligned Irvine-class rocks on Husband Hill (Figure 1a) represent a dike, this
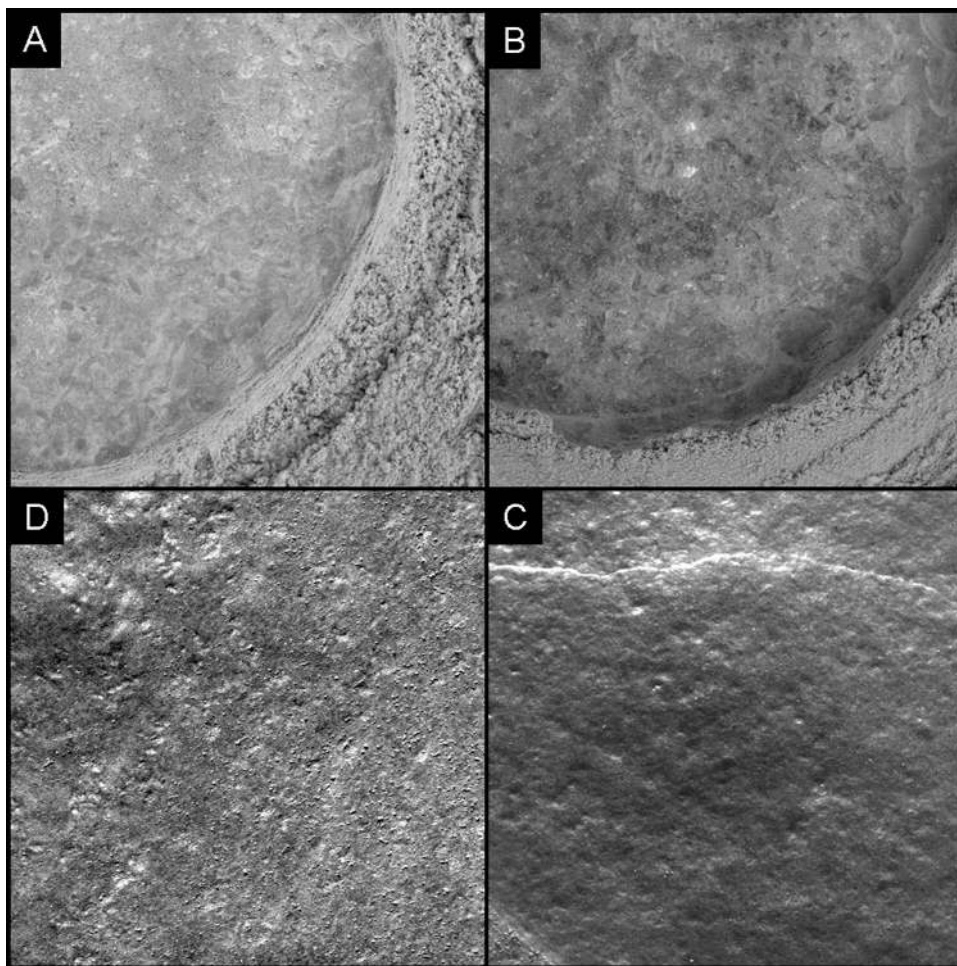
Figure 2. MI focal section merge of (a) Wishstone (3 cm across) and (b) Champagne (3 cm across) after RAT grinding. Note angular grains or clasts. (c) MI image of Irvine, unbrushed (19 mm high). (d) MI image of Backstay, brushed (19 mm high). MI images in Figures 2a and 2b were taken in full shadow, whereas Figures 2c and 2d are illuminated from the top and have been radiometrically calibrated.

would favor a local source for volcanism under Gusev crater itself, and might suggest that Adirondack-class basalts also erupted from local fissures.

4. Spectroscopy

4.1. Thermal Infrared Emission Spectra

[10] Backstay-, and Irvine-class rocks are visually similar in many respects to Adirondack-class rocks and were first recognized as distinct rock types by their MiniTES spectra (Figure 3). Wishstone-class rocks are more rounded, with rougher and lighter-toned surfaces. Some Adirondack-class basalts also occur as float in the Hills, but these are readily distinguished by their thermal emission spectra. The distinguishing spectral features of these four types of float are evident despite the dust on the pointing mirror. Nevertheless, a preliminary correction for the dust contamination [*Ruff et al.*, 2006] has been applied to the spectra of Backstay and Irvine; this correction is unnecessary for Wishstone-class rocks whose spectra were obtained before the dusting event. The low wave number region ($<\sim$600 cm^{-1}) is least affected by dust, and even without such a correction is revealing of the differences among these rock classes. The shape,

position, and magnitude of the dominant emissivity peak in this spectral range varies between the four classes (Figure 3) but is quite invariant within a given class [*Ruff et al.*, 2006]. Even though the middle spectral range ($\sim$750–1250 cm^{-1}) is more susceptible to contributions from dust in the atmosphere and on the mirror, the spectral differences between the classes are clearly evident (Figure 3).

4.2. Visible/Near-Infrared Spectra

[11] The Pancam spectra for Wishstone-class rocks were previously presented in Figure 13 of *Farrand et al.* [2006] and are not reproduced here. These rocks have reflectance maxima at 754 nm (this maximum in Adirondack-class rocks tends to occur at 673 nm), and a long-wavelength band minimum at 934 nm with a steep slope from 754 to 864 nm.

[12] Pancam spectra of Backstay (Figure 4a) reveal four different color units: (1) a bright reddish, dusty surface ("Dusty Rock 1"), (2) a bright bluish, dust-covered, and specularly-reflecting surface ("Dusty Rock 2"), (3) a dark, low-dust surface ("Unbrushed Rock"), and (4) the very dark RAT-brushed region ("Brushed Rock"). Additional
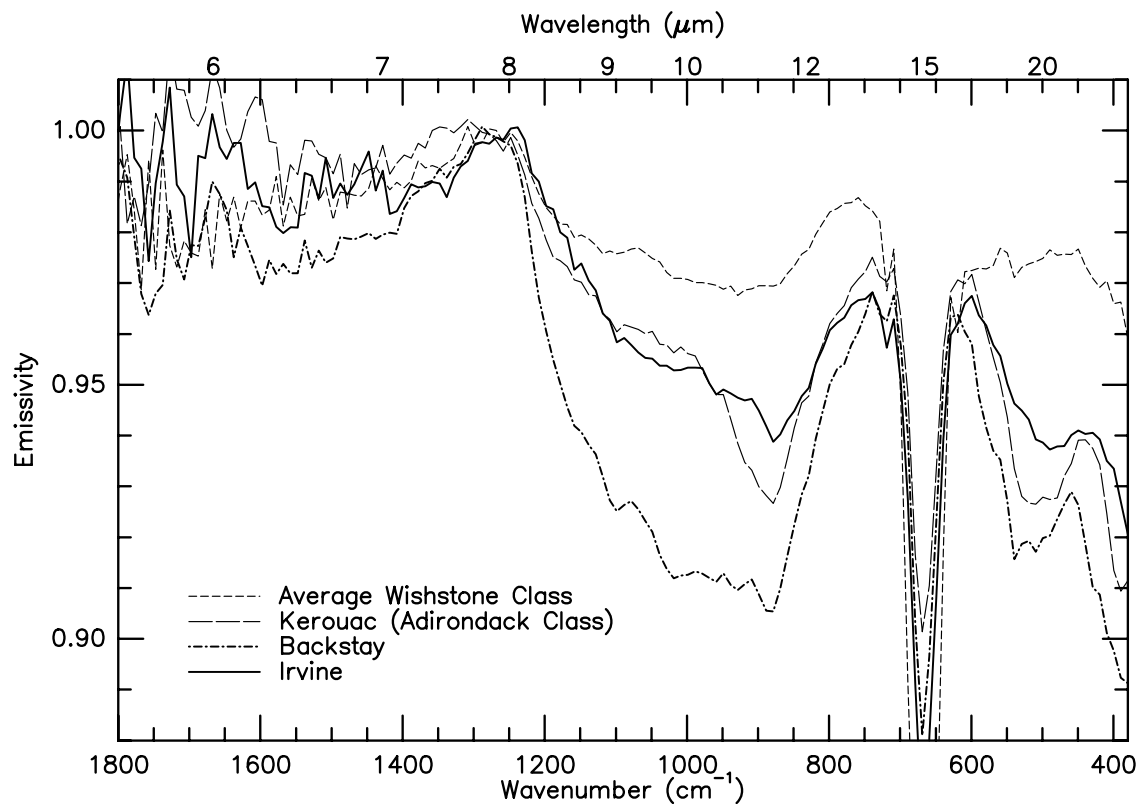
Figure 3. MiniTES spectra of Backstay, Irvine, and the average of four Wishstone-class rocks compared to Adirondack-class spectra, here represented by the float rock Kerouac.

color units identified in the scene adjacent to Backstay are (5) bright reddish dusty soil ("Dust") and (6) dark granular soil ("Dark Soil"). Brushed Backstay is among the lowest albedo rock materials ever seen at Gusev. Indeed, Brushed Rock material is even darker than the brushed and RATed parts of the Adirondack-class basalts studied by *McSween et al.* [2004, 2006]. There is only a weak increase in reflectivity from blue to red wavelengths, indicating little, if any,

contamination of the spectrum by ferric-rich dust. However, the presence of a small amount of dust coating even the "cleanest" looking parts of Backstay (except for the spot brushed by the RAT) is supported by the fact that the Unbrushed Rock spectrum appears to be an approximately 3:1 mixture of Brushed Rock and Dust end-members, assuming these components mix linearly. Similarly, the Dusty Rock 1 spectrum also appears to be a mixture of
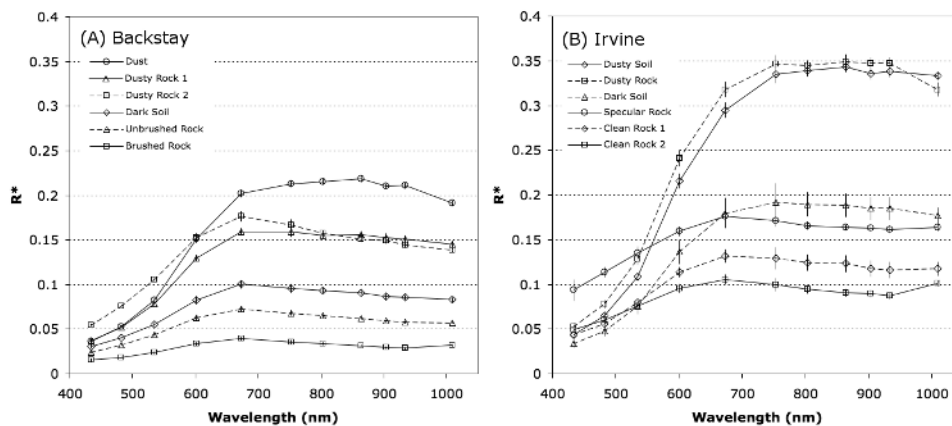

Figure 4. Pancam 11-color spectral units from multispectral imaging of Backstay and Irvine. (a) Spectra of Backstay from Spirit sol 511, Pancam sequence P2563. (b) Spectra of Irvine and surrounding rocks from Spirit sol 603, Pancam sequence P2577. R* is the relative reflectance as defined by *Bell et al.* [2006]. All spectra represent averages from regions of interest consisting of at least 10 to more than 100 pixels on the material indicated in the legends. Error bars represent the standard deviation of the pixel R* values within each region of interest at each wavelength.

Table 1. Chemical Compositions (APXS) and CIPW Norms for Rocks

	Backstay Brushed	Backstay[a]	Irvine Unbrushed	Irvine[a]	Wishstone[a]	Champagne[a]
			Oxides, wt.%			
SiO_2	49.5	49.6	47.0	46.6	44.4	44.0
TiO_2	0.93	0.93	1.06	1.05	2.63	3.02
Al_2O_3	13.3	13.3	10.6	10.5	15.2	15
Fe_2O_3[b]	3.32	3.33	7.68	7.61	5.23	6.33
Cr_2O_3	0.15	0.15	0.20	0.20	0.00	0.00
FeO[b]	10.7	10.7	12.3	12.2	7.05	6.96
MnO	0.24	0.24	0.36	0.36	0.22	0.25
MgO	8.31	8.32	10.6	10.5	4.56	4.01
CaO	6.04	6.05	6.03	5.98	9.01	8.88
Na_2O	4.15	4.16	2.68	2.66	5.07	5.07
K_2O	1.07	1.07	0.68	0.67	0.58	0.54
P_2O_5	1.39	1.39	0.97	0.96	5.26	5.12
SO_3	1.52	0.75	2.37	0.75	0.75	0.75
Cl	0.35	0.00	0.45	0.00	0.00	0.00
Total	101.0	100.0	103.0	100.0	100.0	100.0
			Norms, wt.%			
qtz						0.49
cor					2.4	2.2
feldspars		56.0		41.2	56.7	56.7
or		6.3		4.0	3.4	3.2
ab		35.2		22.5	42.9	42.9
an		14.5		14.7	10.4	10.6
di		5.3		7	0.0	0.0
hy		11.9		29.9	13.5	13.0
ol		16.0		5.6	1.9	0.0
fo		8.7		3.4	1.3	0.0
fa		7.3		2.2	0.6	0.0
mt		4.8		11.0	7.6	9.2
cr		0.2		0.3	0.0	0.0
ilm		1.8		2.0	5.0	5.7
ap		3.3		2.3	12.5	12.1

[a]Preferred composition, adjusted to 0.75% SO_3 (0.3% S) and 0% Cl, and normalized to 100%.
[b]Fe partitioning between oxidation states based on Mössbauer determinations of Fe^{3+}/Fe_{Total} = 0.23 for Backstay, 0.36 for Irvine, 0.40 for Wishstone, and 0.45 for Champagne [*Morris et al.*, 2006].

Brushed Rock and Dust end-members, but in approximately the opposite 1:3 ratio.

[13] Pancam spectra of Irvine (Figure 4b) and its associated rocks reveal four primary color units: (1) bright reddish dusty surfaces ("Dusty Rock"), (2) bright bluish, low-dust, and specularly-reflecting surfaces ("Specular Rock"), (3) dark and only moderately dusty surfaces ("Clean Rock 1"), and (4) the darkest, lowest-dust surfaces ("Clean Rock 2"). None of the locations of spectral measurements corresponds to the APXS and MB measurements, but that rock face was selected for its low dust appearance. Two additional color units were identified in the Irvine scene: (5) bright reddish dusty soil ("Dusty Soil") and (6) dark granular soil ("Dark Soil"). A small amount of dust appears to coat the Irvine Clean Rock 1 surfaces, inferred primarily from the stronger short wavelength ferric absorption edge in their spectra relative to the darker Clean Rock 2 surfaces. The Specular Rock class appears to be spectrally similar to the Clean Rock 2 class, but with a higher reflectivity. These are probably the same rock materials as Clean Rock 2 surfaces, but are brighter at all wavelengths because of mirror-like glinting of sunlight from specularly-oriented facets.

5. Geochemistry

[14] APXS chemical analyses of Backstay, Irvine, Wishstone, and Champagne are presented in Table 1. The

Backstay, Wishstone, and Champagne compositions were previously discussed by *Ming et al.* [2006], but Irvine was not included in that paper's timeframe. The compilation of APXS analyses by *Gellert et al.* [2006] included Wishstone and Champagne, but not Backstay or Irvine. Since the Backstay and Irvine compositions have not been previously published, the full APXS analyses are included in Table 1. Preferred rock compositions, indicated by footnoted headings in Table 1, were produced by partitioning iron between FeO and Fe_2O_3 on the basis of Fe^{3+}/Fe_{Total} ratios determined by MB measurements (Table 1, footnote). To correct for any adhering dust, the preferred compositions of all rocks were adjusted to 0.75 wt.% SO_3 (corresponding to 0.3 wt.% sulfur, the average for basaltic Martian meteorites which contain iron-sulfides) and 0 wt.% chlorine, and renormalized to 100%. Similar adjustments were also made to derive the compositions of Adirondack-class basalts [*McSween et al.*, 2004, 2006].

[15] CIPW norms calculated using MB-derived Fe^{3+}/Fe_{Total} ratios (Table 1) suggest that the rocks are composed mainly of plagioclase, pyroxenes (predominantly hypersthene), and lesser olivine. All rocks contain considerable amounts of normative apatite and Fe-Ti-Cr oxides (magnetite, ilmenite, and chromite in Backstay and Irvine; ilmenite and magnetite in Wishstone and Champagne). Normative olivine compositions are ferroan (Fo_{61} for Irvine, Fo_{55} for Backstay, Fo_{69} for Wishstone, Fo_{46} for Champagne) and

Table 2. Fe Mineralogy of Rocks Determined by Mössbauer

	Mössbauer Measurements (area/Fe atoms in each phase)[a]				
	A(Ol)	A(Px)	A(Ilm)	A(Mt)	A(Hm + npOx)
Humphrey	49	31	0	14	6
Irvine	10	46	0	35	4
Backstay	35	37	3	11	2
Wishstone	20	29	8	12	30
	Renormalized Modal Fe Mineralogy,[b] wt.%				
	Ol	Px	Ilm	Mt	Hm
Humphrey	30	25	0	4	2
Irvine	6	39	0	10	1
Backstay	15	22	1	2	0.4
Wishstone	7	14	2.5	2	5

[a]Humphrey (postgrind) data from *Morris et al.* [2004], Backstay (postbrush) data from *Morris et al.* [2006], Irvine (unbrushed) data not previously published.

[b]Each area (representing the proportion of Fe atoms in each phase) is divided by the number of Fe atoms per formula unit for that phase, then multiplied by the molecular weight of that phase, and then renormalized to 100% after correcting for the proportions of plagioclase + apatite (not analyzed by MB) in the calculated norm for that rock (*McSween et al.* [2006] for Humphrey, Table 1 for other norms). Nanophase oxides (npOx) were combined with Hematite (Hm).

similar to those in Adirondack-class basalts [*McSween et al.*, 2006]. The compositions of normative plagioclase are richer in alkalis ($An_{36}Ab_{54}Or_{10}$ for Irvine, $An_{27}Ab_{62}Or_{11}$ for Backstay, $An_{18}Ab_{76}Or_6$ for Wishstone, $An_{19}Ab_{76}Or_5$ for Champagne) than Adirondack-class rocks ($An_{46}Ab_{52}Or_2$ for Humphrey [*McSween et al.*, 2006]) and are similar to feldspar compositions in some terrestrial alkaline lavas [*Nekvasil et al.*, 2000]. The norm calculation procedure does not include amphiboles, nor does it recognize the occurrence of coexisting feldspars; both are common in terrestrial alkalic rocks.

6. Mineralogy

6.1. Mineralogical Interpretation of MB Spectra

[16] MB measurements of Wishstone, Irvine, and Backstay (Table 2) show that pyroxene and olivine occur, as well as Fe-oxides (magnetite, hematite, nanophase oxides, and in the case of Backstay and Wishstone, ilmenite). MB spectroscopy has a greater penetration depth than visible/near-infrared spectra, so a very thin dust coating seen in Pancam data may have no effect on MB; in general, MB spectra of Gusev plains basalts are quite similar for unbrushed, brushed, and RATed surfaces [*Morris et al.*, 2006].

6.2. Comparison of MB Results and Normative Mineralogy

[17] Mössbauer results can be compared with normative mineralogy (Table 1) if suitable corrections are applied. MB relative peak areas (A, Table 2) assigned to iron atoms in specific phases were converted to approximate wt.% minerals, and then renormalized to take into account the normative proportions (wt.%) of Fe-free minerals (plagioclase and apatite) not detected by Mössbauer spectroscopy (see footnote in Table 2). Nanophase iron oxides were assumed to be highly oxidized and were combined with hematite. The agreement between normative mineral abundances and MB-determined mineral modes (Table 2) is

remarkable (Figure 5). The high abundances of MB-determined magnetite in Irvine and hematite in Wishstone correspond to their high Fe^{3+}/Fe_{Total} (Figure 5). It is not clear whether the high magnetite content of Irvine is primary or results from postmagmatic oxidation. The high hematite proportion in Wishstone may be an artifact of weathering, although rocks of this class are thought to be less altered than outcrops in the Hills [*Morris et al.*, 2006].

6.3. Mineralogical Interpretation of Pancam Spectra

[18] The mineralogy inferred from the calculated norm and MB spectra of Backstay (Figure 5) is also consistent with interpretations of Pancam spectra. The peak in reflectivity near 673 nm, the decrease in reflectivity from 673 to 1000 nm, and the evidence for a weak, broad absorption feature in the spectrum centered between 860 nm and 930 nm (Figure 4a) argue for the existence of a ferrous iron phase such as low-Ca pyroxene (orthopyroxene or pigeonite), based on previous laboratory and Mars spectroscopic studies [e.g., *Adams*, 1974; *Mustard and Sunshine*, 1995]. Olivine may also contribute to the negative near-IR spectral slope, but given the limited near-IR spectral coverage of the Pancam instrument, details about potential olivine cannot be uniquely identified or constrained. The upturn in the Pancam spectra of Backstay at the longest wavelengths, however, indicates that this rock likely has a higher ratio of pyroxene to olivine than Adirondack-class basalts [*McSween et al.*, 2004] and anomalous olivine- or pyroxene-bearing basaltic fragments found at the Mars Pathfinder site [*Bell et al.*, 2002]. In addition, the extremely low reflectivity of Backstay compared to other rocks at Gusev is consistent with the presence of an additional opaque mineral phase or phases, such as magnetite or ilmenite.

[19] Pancam spectra of Irvine Clean Rock 2 surfaces exhibit a reflectivity maximum near 673 nm and a well defined, though weak near-IR absorption feature centered near 900 to 930 nm (Figure 4b). Spectra of Clean Rock 1
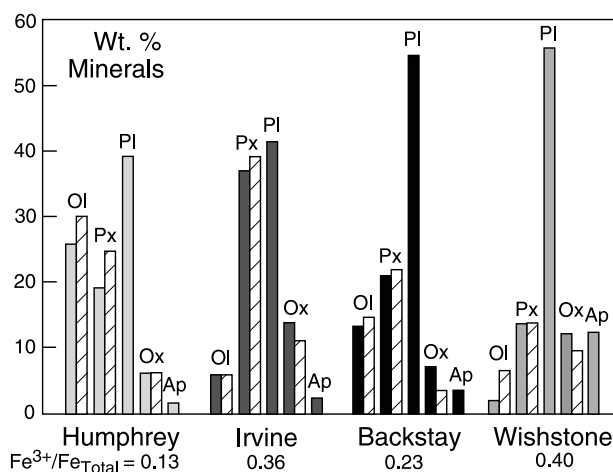

Figure 5. Comparison of normative mineral abundances (shaded bars, Humphrey from *McSween et al.* [2006]; Irvine, Backstay, and Wishstone from Table 1) and Mössbauer-derived mineral abundances (hatched bars, *McSween et al.* [2006] and Table 2) for the RATed surface of Humphrey, an unbrushed surface of Irvine, a brushed surface of Backstay, and RATed Wishstone.
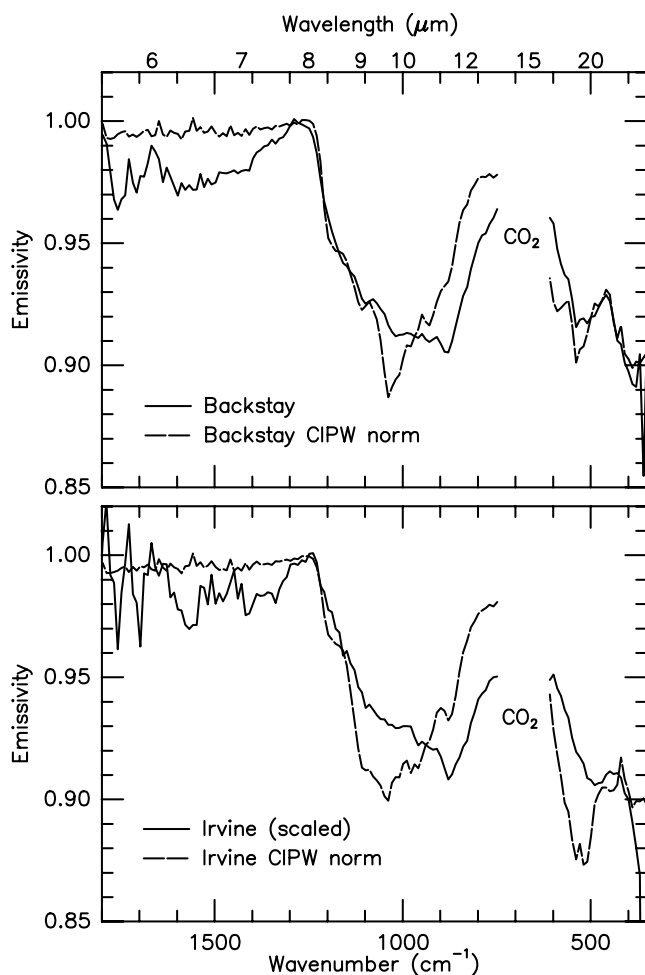
Figure 6. Calculated MiniTES spectra for rocks having the normative mineralogy of Backstay and Irvine (Table 1), compared to measured spectra. The poor fits suggest missing or improperly modeled component(s), perhaps glass and/or pigeonite.

surfaces are similar, though with a less well-defined near-IR absorption feature because of the apparent admixture of a small amount of dust covering these surfaces. These spectra exhibit either flat or only weakly negative spectral slopes in the 673 to 1000 nm region. Similar to Backstay, these properties of Irvine-class rocks, combined with their moderately low albedo and lack of a strong ferric absorption feature in the 430 to 673 nm region, are consistent with the presence of orthopyroxene or pigeonite. The spectral behavior of these rocks in the near-infrared indicates that they also probably have a much higher ratio of pyroxene to olivine than Adirondack-class basalts [*McSween et al.*, 2004, 2006] and Backstay. The reflectivity of Irvine Clean Rock surfaces is comparable to those of unbrushed surfaces of Adirondack, Humphrey, and Mazatzal, none of which are as dark as the Unbrushed Rock surface of Backstay. Thus there is no evidence in Pancam spectra for additional opaque mineral phases in Irvine.

[20] Pancam spectra of Wishstone also support the mineralogy inferred from the calculated norm and MB data [*Farrand et al.*, 2006]. In particular, the dominance of

low-Ca pyroxene (orthopyroxene or pigeonite) over olivine is suggested by the upturn in the Pancam spectra of Backstay at the longest wavelengths.

6.4. Mineralogical Interpretation of MiniTES Spectra

[21] MiniTES spectra of Wishstone and many other rocks of this class were obtained before the pointing mirror was contaminated with dust, and distinctive low wave number features are evident. Deconvolution of a subset of four averaged Wishstone-class spectra [*Ruff et al.*, 2006] yielded the following mineralogy: 55% plagioclase, 15% olivine (Fo_{30-40}), 10% basaltic glass, 10% phosphate (wavellite?), and 10% sulfate. Ilmenite was also inferred from the APXS analyses, but inclusion of this phase in the spectral end-member set does not change the modeled components or improve the RMS error. This mineralogy is similar to that determined by MB and norm (Figure 5), except that the MiniTES olivine abundance is higher and there is no pyroxene component (pyroxene appeared in deconvolutions without sulfate, however [*Ruff et al.*, 2006]). A small surface dust component (~10%) is present in all the deconvolutions.

[22] Deconvolution analysis of MiniTES spectra of Backstay and Irvine must await a robust and quantitative correction for dust on the pointing mirror. Until then, a partial assessment of the mineralogy of these rocks may be possible using the CIPW norms calculated above (Table 1). The norms were converted to thermal emission spectra using the correct proportions of library spectra that simulate the normative components, and the synthetic spectra were then compared to measured spectra. Such a strategy was successfully employed in the analysis of Adirondack-class basalts [*Ruff et al.*, 2006]. However, the norm-derived spectra of Backstay and Irvine are poor matches to the measured spectra (Figure 6). One possible explanation is that both rocks contain glass, which is not accounted for in the norm calculation. However, basaltic glass has a MB spectrum like that of pyroxene, so in that case we would expect to see higher MB-determined pyroxene, but the pyroxene abundance from MB data matches the normative pyroxene for both rocks (Figure 5). Another possibility is that pigeonite in the spectral library is not a suitable compositional match for the low-Ca pyroxene in these rocks.

7. Rock Classification

[23] Using the total alkalis versus silica classification diagram for volcanic rocks (Figure 7), Wishstone and Champagne are tephrites, Irvine is a basalt, and Backstay is a trachybasalt (subclassification hawaiite, having $Na_2O -$ $2.0 \geq K_2O$ [*Le Maitre*, 2002]). Relative to Adirondack-class basalts (Adirondack, Humphrey, and Mazatzal), all of these rocks have higher alkali contents (Figure 7). The diagonal gray lines in Figure 7 mark the division between alkaline (Alk) and subalkaline (Sub) rocks, according to two different classifications by *Irvine and Baragar* [1971] and *Hyndman* [1972]. Humphrey and Irvine straddle this boundary, and Backstay, Wishstone, and Champagne clearly plot within the alkaline field. Gusev rocks are clearly different in composition from Martian meteorites (SNCs), the Mars Pathfinder dust-free rock, and Mars
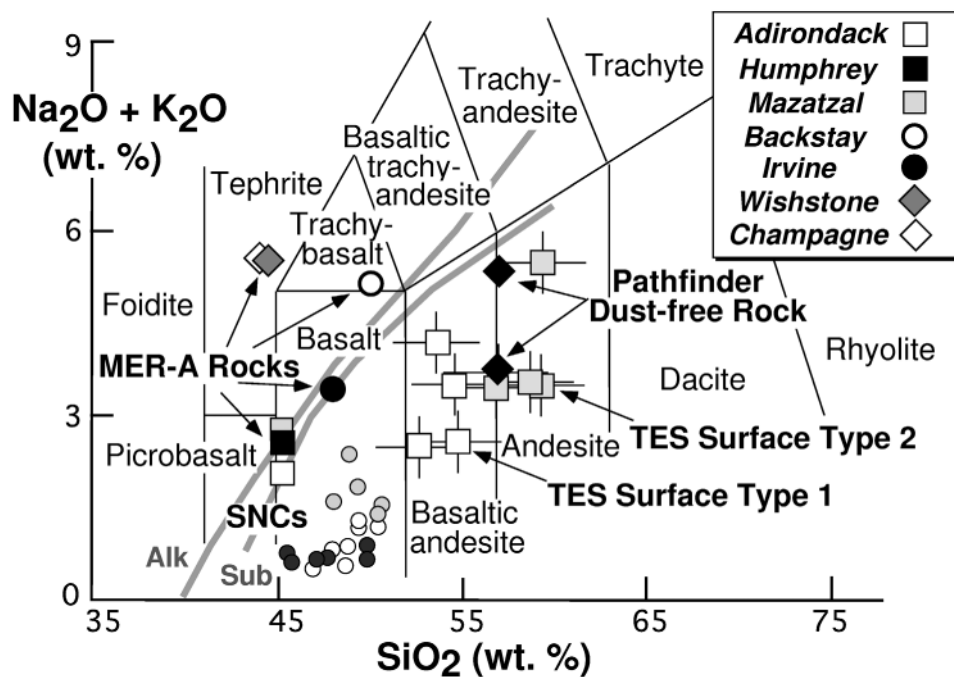
Figure 7. Alkalis versus silica classification diagram for volcanic rocks [*Le Bas et al.*, 1986] shows APXS analyses of Gusev (MER-A) rocks and other analyses of Martian samples. Gray lines indicate the boundary between alkaline (Alk) and subalkaline (Sub) rocks, according to *Irvine and Baragar* [1971] and *Hyndman* [1972]. Adirondack, Humphrey, and Mazatzal [*McSween et al.*, 2006] are RATed plains basalts, Backstay (brushed) and Irvine (unbrushed) (Table 1) are basaltic rocks from the Columbia Hills, and Champagne and Wishstone [*Gellert et al.*, 2006; *Ming et al.*, 2006] are additional float samples from the Hills. Error bars are generally smaller than the symbols. Two calibrations of the Mars Pathfinder dust-free rock [*Wänke et al.*, 2001; *Foley et al.*, 2003] are shown. SNC meteorite compositions (small circles) include basaltic shergottites (dark gray), olivine-phyric shergottites (light gray), and nakhlites (unfilled) (data sources of *McSween et al.* [2003]). TES surface compositions are estimated from various mineral deconvolutions [*McSween et al.*, 2003, and references therein].

surface compositions inferred from orbital thermal emission spectroscopy (Figure 7).

8. Petrogenesis

[24] On Earth, some "hot spot" magmatic suites such as those found on oceanic islands (e.g., Ascension, Azores, Samoa) and in continental hot spot (e.g., Nandewar volcano, Australia) and rift sequences (e.g., Kenya), are mildly alkaline but without the strong undersaturation in silica that characterizes many alkalic provinces [*Nekvasil et al.*, 2004, and references therein]. The mildly alkaline compositions of Irvine and Backstay are somewhat similar to those rocks (the compositions of Nandewar lavas are illustrated by the shaded field in Figure 8). As described by *Nekvasil et al.* [2004], the magmatic evolution of Nandewar and other mildly alkaline centers is characterized by strong increase in alkalis relative to silica in basaltic members and its moderation at intermediate compositions. These magmas are thought to originate through fractional crystallization, although difficulties are encountered when modeling melt evolution by extracting the phenocryst assemblage [e.g., *Stolz*, 1985]. Experiments by *Nekvasil et al.* [2004] confirmed that fractionation of the Nandewar phenocryst assemblage did not yield the liquid line of descent, but high-pressure fractionation of olivine, ortho-

pyroxene, clinopyroxene, kaersutite, apatite, ilmenite, and late plagioclase could produce this magmatic sequence. Their model of deep-seated fractionation allows later low-pressure crystallization (without crystal separation, producing the phenocryst assemblage) during ponding nearer the surface. The critical parameter in producing alkalic magmas is suppression of plagioclase crystallization in favor of a pyroxene-dominated assemblage, accomplished by high pressure and water content, although mildly alkaline magmas might arise by fractionation at lower pressures.

[25] The composition of Adirondack-class rocks is thought to represent that of a primary liquid, based on experiments that demonstrate its multiple saturation with olivine + orthopyroxene + spinel at ~1.0 GPa (~85 km depth) [*Monders et al.*, 2006]. Thus it is plausible that the Adirondack-class magma could be parental to fractionated magmatic rocks in Gusev. Some Adirondack-class rocks contain abundant vesicles [*McSween et al.*, 2006] and other rocks encountered by Spirit are scorias or volcano-clastic deposits, suggesting that some Gusev magmas had relatively high volatile contents. The redox state of Adirondack-class rocks is estimated to lie near the quartz-fayalite-magnetite (QFM) buffer, as appropriate for the MB-determined Fe^{3+}/Fe_{Total} (0.16) for Humphrey [*McSween et al.*, 2004].
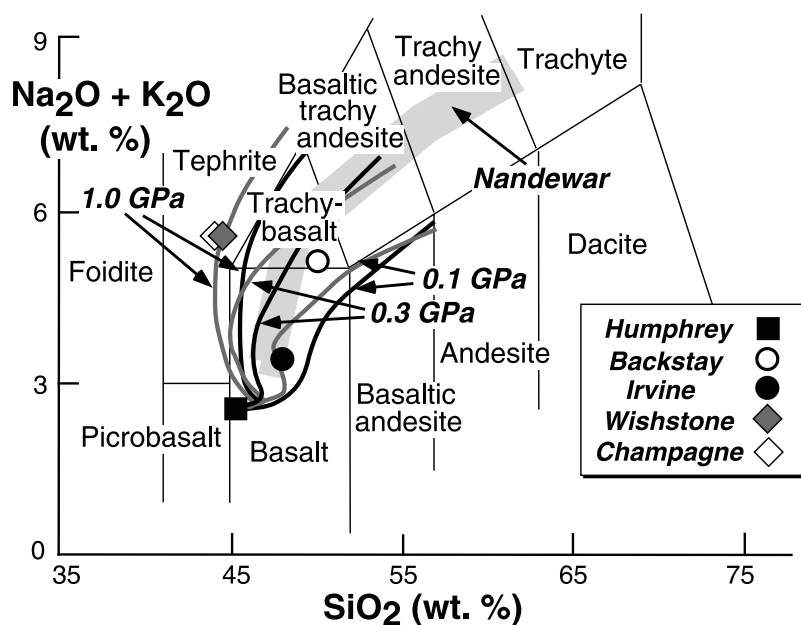
Figure 8. Alkalis versus silica diagram showing the compositions of Humphrey, Irvine, Backstay, Wishstone, and Champagne. The heavy gray band is the fractionation trend of alkalic rocks from the Nandewar volcano [*Nekvasil et al.*, 2004]. Thin black curves illustrate the evolution of liquids produced by equilibrium crystallization, and thin gray curves are melts arising from fractional crystallization. All liquid lines of descent are calculated using MELTS for a Humphrey rock composition [*McSween et al.*, 2006] with 0.5 wt.% H_2O. Liquid lines of descent are calculated at QFM or QFM-1. The 0.1 GPa fractionation path passes through the composition of Irvine, and the Backstay composition is bracketed by the 0.1 and 0.3 GPa fractionation paths. A liquid line of descent at high pressure (1.0 GPa) produces compositions like Wishstone and Champagne.

[26] Illustrated in Figure 8 are liquid lines of descent for equilibrium (black) and fractional (gray) crystallization of an Adirondack-class melt composition (Humphrey [*McSween et al.*, 2004], with an assumed water content of 0.5 wt.% H_2O), calculated using MELTS [*Ghiorso and Sack*, 1995]. The liquid paths at 0.1 and 0.3 GPa are at an oxidation state corresponding to the QFM buffer, and those at 1.0 GPa are one log unit more reducing (QFM-1). QFM-1 may be more appropriate at high pressure because magma redox state is expected to become more reducing with increasing depth [*Ballhaus and Frost*, 1994]. The fractional crystallization path at 0.1 GPa passes through the composition of Irvine on this diagram. The composition of Backstay is bracketed by the fractional (and equilibrium) crystallization paths at 0.1 and 0.3 GPa. These observations suggest that fractionation of Adirondack-class magma at modest pressures might account for both of these rock compositions. In contrast, high-pressure fractionation at 1.0 GPa may produce Wishstone-class magmas (Figure 8).

[27] Figure 9 compares the abundances of other oxides in Humphrey, Irvine, Backstay, and Wishstone with the QFM and QFM-1 liquid lines of descent calculated from MELTS at various pressures. Also illustrated by shaded fields are rock compositions from the Nandewar volcano [*Nekvasil et al.*, 2004]. Nandewar rocks are geochemically distinct from these Martian rocks, but some Humphrey-Irvine-Backstay trends (decreasing MgO and CaO, increasing P_2O_5, flat Al_2O_3, with increasing SiO_2) mimic the terrestrial trends. The 0.1 GPa fractionation path passes through or near the Irvine composition for all components except CaO. The

Backstay composition plots between the 1.0 and 0.3 GPa fractionation paths, except for MgO and P_2O_5. The 1.0 GPa paths are consistent with the Wishstone composition except for TiO_2, P_2O_5, and FeO* (Figure 9).

[28] The order of crystallization and proportions (g/100 g liquid) of fractionated minerals in the MELTS calculations are shown in Figure 10. Increasing pressure from 0.1 to 0.3 GPa decreases the proportion of olivine relative to low-Ca pyroxene and suppresses the crystallization of phosphate. Early-crystallizing spinels at low pressures are chromite-spinel solutions, whereas later-crystallizing spinels are magnetite. At 1.0 GPa, olivine no longer appears, and garnet (almandine-grossular-pyrope solution) replaces plagioclase until late in the fractionation sequence. Chromite-spinel gives way to ulvospinel-magnetite at lower temperatures, allowing TiO_2 to increase initially, but not to the degree necessary to explain the high TiO_2 content of Wishstone (Figure 9). The late crystallization of magnetite also explains the increase in FeO* (Figure 9). Whitlockite crystallizes early in this model, so P_2O_5 does not increase (unlike Wishstone, as seen in Figure 5). The high TiO_2 and P_2O_5 and low FeO* values of Wishstone constitute the most serious discrepancies for the high-pressure fractionation model. Use of the program pMELTS at 1.0 GPa likewise does not reproduce liquid lines of descent having the high TiO_2 and low FeO* values of Wishstone, but it does produce high P_2O_5 values. These discrepancies may reflect accumulation of oxide and phosphate minerals in Wishstone, perhaps by aerodynamic sorting of ash components. Alternative explanations may be varying degrees of partial melting to produce
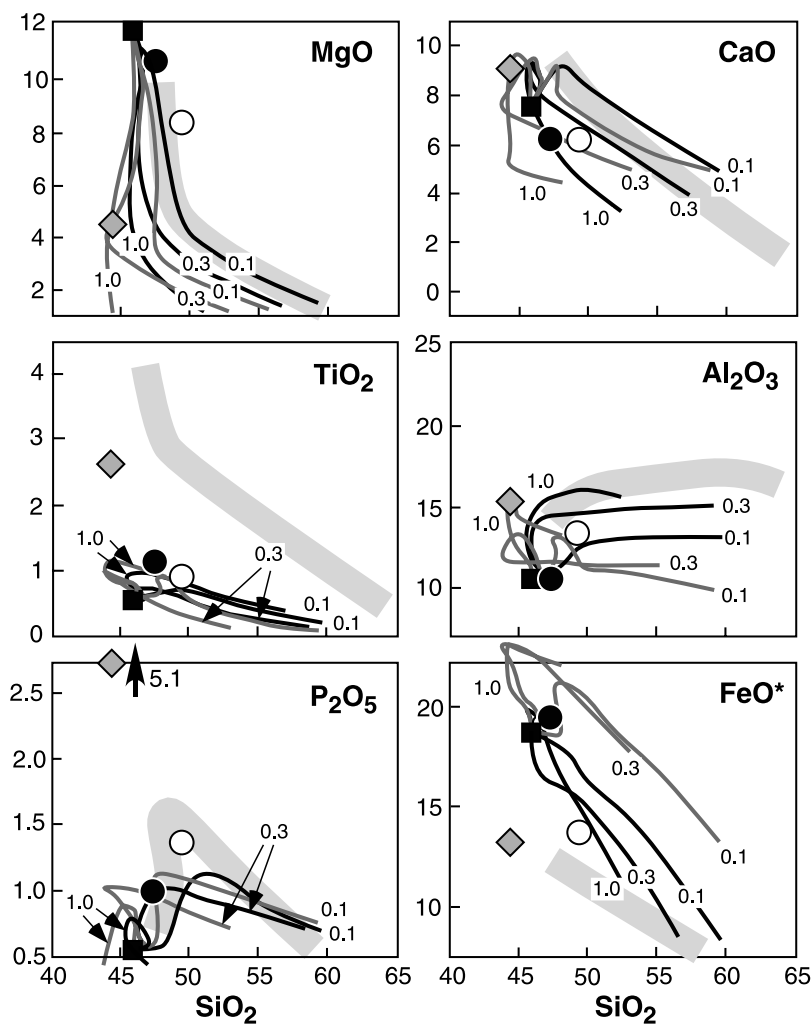
Figure 9. Plots of other oxides versus silica for Humphrey, Irvine, Backstay, and Wishstone (symbols as in Figure 7). Lines represent the liquid lines of descent calculated for Humphrey using MELTS at QFM and QFM-1, and gray bands are alkalic rocks from the Nandewar Volcano [*Nekvasil et al.*, 2004].

the parent magma, mantle source heterogeneity, or crustal assimilation. The fractionation models proposed here require validation by crystallization experiments, because these magma compositions may lie outside the range of liquids used to calibrate MELTS.

[29] Trends of Ni-Mg and Cr-Mg (Figure 11) are distinctive for Martian meteorites [*Wänke and Dreibus*, 1988]. Adirondack-class basalts plot near but not directly on these trends [*McSween et al.*, 2006]. Wishstone, Champagne, Backstay, and Irvine plot farther off the SNC Ni-Mg trend (Figure 11a). Backstay and Irvine plot directly on the Cr-Mg trend (Figure 11b), but Wishstone-class rocks contain no detectable chromium. Nickel is strongly partitioned into olivine, but the trend in the measured Ni concentrations (Irvine 289 ppm > Backstay 228 ppm > Humphrey 164 ppm > Wishstone 40 ppm, with uncertainties typically >10%) bears no obvious relationship to the amounts of olivine predicted to have fractionated to form these rocks (Figure 10). Other rocks from the Columbia Hills also have unexplained high Ni concentrations [*Ming et al.*, 2006]. Chromium is partitioned into spinel, and its depletion in Irvine, Backstay, and especially Wishstone relative to Humphrey (Figure 10b)

is consistent with MELTS calculations that predict early crystallization of chromian spinel and the higher Cr contents of high-pressure spinels.

[30] We hypothesize that Irvine and Backstay may be melts derived by fractional crystallization of primitive picritic basaltic magmas that were compositionally similar to those found on the Gusev plains (the Adirondack class). These mildly alkaline magmas fractionated at varying pressures, presumably during ascent or in crustal reservoirs beneath Gusev crater. MELTS models suggest fractionation at pressures of ∼0.1 GPa for Irvine and ∼0.2 GPa for Backstay. The Wishstone magma is more strongly alkaline and may have formed by fractionation of a similar melt at ∼1.0 GPa. Discrepancies in some elements for the Wishstone model might reflect aerodynamic sorting of ash components. The Irvine- and Backstay-class magmas could have intruded Husband Hill as dikes or sills, whereas the Wishstone-class may have erupted as pyroclastic materials. Alternatively, the fractionated magmas may have extruded elsewhere in the crater and were sampled later by impacts that lofted them onto the Hills. If these rocks are ejecta, they might be older than the Adirondack-class basalts on the
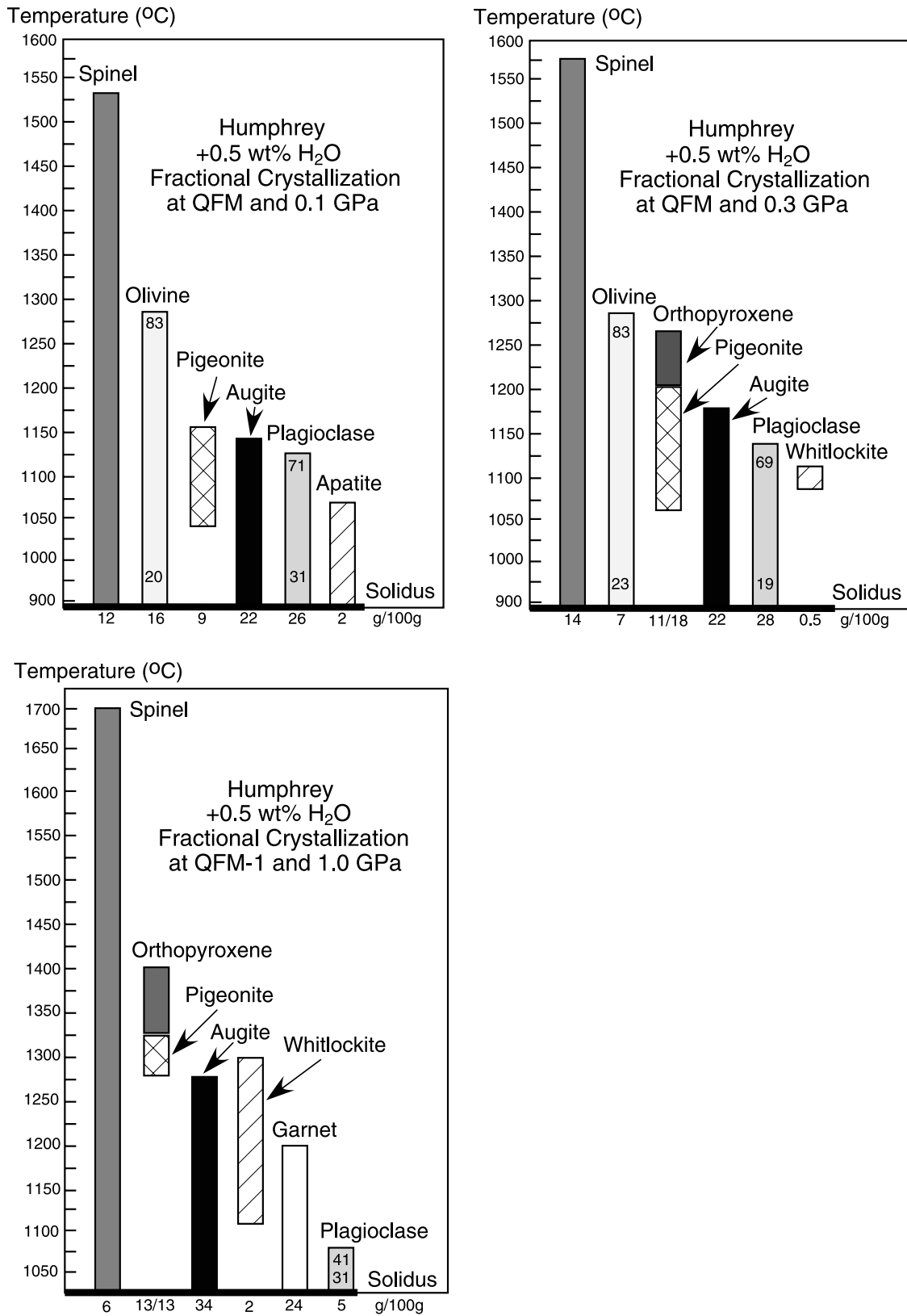
Figure 10. Order of crystallization of minerals in the MELTS liquid lines of descent for Humphrey melt composition calculated at various pressures. Proportions of minerals (expressed as g/100 g magma) are given at the bottom of the figure. Numbers in olivine and plagioclase bars indicate compositions (Fo and An, respectively).
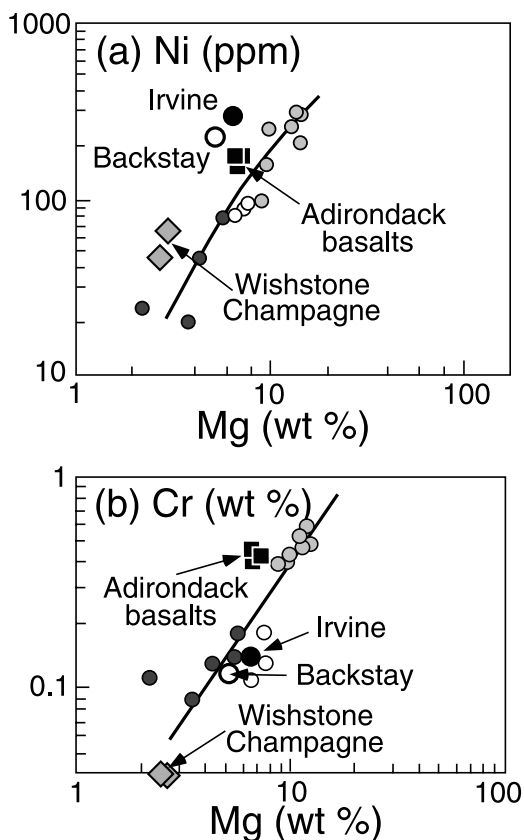
Figure 11. (a) Ni versus Mg and (b) Cr versus Mg in Gusev rocks and Martian meteorites. Symbols for basaltic shergottites, olivine-phyric shergottites, and nakhlites as in Figure 6.

plains (Grant et al., manuscript in preparation, 2006) and thus would have formed by fractionation of earlier magmas that were similar in composition to the Adirondack class. Because the Adirondack-class magma composition represents a primitive liquid [*Monders et al.*, 2006], similar magmas could have formed repeatedly during the life of this volcanic province. Regardless of whether the primitive and evolved magmas were emplaced coevally or at different times during Gusev's magmatic evolution, the lack of alteration suggests that they postdated the hypothesized fluvial events in Gusev crater [*Cabrol et al.*, 1998] and the aqueous alteration of outcrops in the Columbia Hills [*Squyres et al.*, 2006].

[31] Recognizing the alkaline nature of fractionated rocks like Irvine, Backstay, and Wishstone is more obvious than for their parental basalts (Figure 7). These rocks constitute the first definitive discovery of alkaline volcanism on Mars, although there have been previous suggestions of alkalinity in Martian meteorites. *Nekvasil et al.* [2003] hypothesized that the parent magma for Chassigny (a cumulate dunite) was alkalic, and the calculated liquid line of descent for the Nakhla parental magma at low pressure [*Stockstill et al.*, 2005] is similar to that estimated for Gusev basalt (Figure 12). Analyses of intercumulus glasses in the MIL 03346 nakhlite (shown as small black circles in Figure 12) also have alkaline compositions [*Day et al.*, 2006]. However, orbital remote sensing of Mars to date has focused on only subalkaline compositions. The search for strongly alkaline rocks requires the addition of alkali-rich minerals to spectral libraries [e.g., *Dunn and McSween*, 2005]. Mildly alkaline basalts, like those described here, contain essentially the same minerals as in subalkaline basalts, but with different feldspar or glass compositions and in different proportions; such rocks may be difficult to recognize using orbital spectroscopy [*Dunn and McSween*, 2005], but are readily identified by
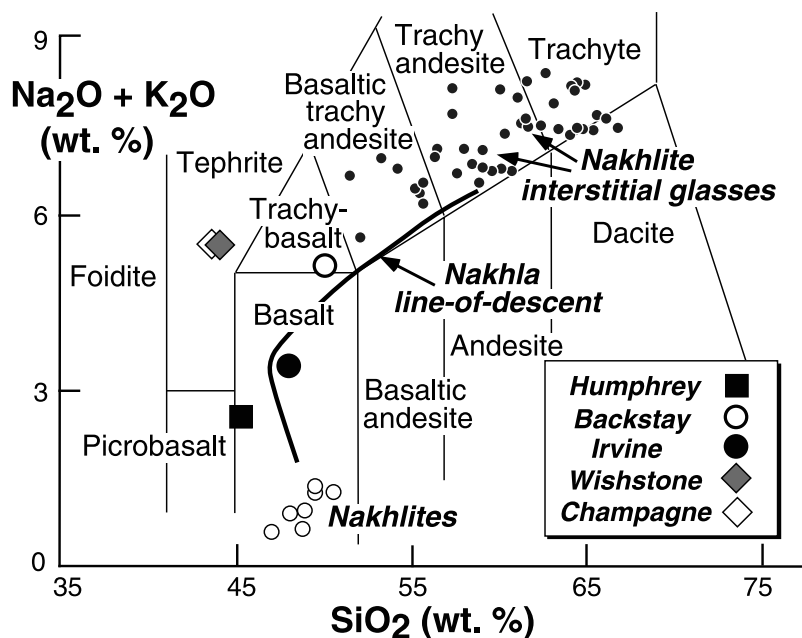

Figure 12. Alkalis versus silica diagram showing the compositions of nakhlites, a MELTS-calculated liquid line of descent for the parental melt of the Nakhla Martian meteorite [*Stockstill et al.*, 2005], and analyses of intercumulus glasses in the MIL 03346 nakhlite [*Day et al.*, 2006].

accurate chemical analyses using instruments on the planet's surface.

9. Summary

[32] Relatively unaltered float rocks encountered by the Spirit rover in the Columbia Hills are distinguished as members of the Wishstone, Irvine, and Backstay classes. Detailed observations and analyses of the type specimens for these classes using the Athena instrument package have allowed more thorough characterization of these rocks:

[33] 1. All these rocks, as well as other samples of their classes, occur as float on the flank of Husband Hill, but were not encountered on the Gusev plains. Alignment of Irvine-class rocks at one location may suggest that they represent a dike or sill, but this is conjectural.

[34] 2. Irvine and Backstay have low albedos, and all these rocks have been eroded by eolian particles. MI images of RAT-ground Wishstone show a clastic texture of small, angular grains, as appropriate for a pyroclastic rock. Backstay and Irvine are aphanitic and featureless, except for some small knobs on Backstay and some pits seen in MI images of both rocks, and are interpreted as lavas or dike rocks.

[35] 3. MiniTES spectra readily distinguish among the various classes of basaltic rocks observed on Husband Hill and have allowed for an accounting of their relative abundances and distributions.

[36] 4. APXS analyses indicate that Wishstone, Irvine, and Backstay have alkalic compositions. Wishstone is chemically classified as tephrite, Irvine as an alkaline basalt, and Backstay as trachybasalt (hawaiite).

[37] 5. Normative calculations suggest the rocks are composed of sodic plagioclase (An_{18-36}, with high K_2O), pyroxenes (mostly hypersthene with some high-Ca pyroxene except in Wishstone, ferroan olivine (Fo_{69-61}), Fe-Ti-Cr oxides (magnetite and ilmenite, plus chromite in Backstay and Irvine), and apatite (especially abundant in Wishstone).

[38] 6. MB measurements show the presence of Fe-bearing olivine, pyroxene, and oxides (magnetite, ilmenite, hematite, and nanophase ferric oxide). The relative proportions of these phases, when adjusted for other minerals not detected by MB, agree remarkably well with normative mineral modes.

[39] 7. Pancam visible/near-infrared spectra are consistent with the presence of abundant low-Ca pyroxene (orthopyroxene or pigenonite) and less olivine than in Adirondack-class rocks. Opaque minerals are inferred in Backstay spectra, but curiously not in Irvine spectra. Deconvolution of MiniTES spectra for Wishstone-class rocks suggest plagioclase, olivine, glass, phosphate, and sulfate. MiniTES spectra for Irvine and Backstay cannot be deconvolved, but synthetic thermal emission spectra calculated using the normative mineralogy for Backstay and Irvine provide poor matches to measured MiniTES spectra, possibly suggesting the presence of some glass or pigeonite.

[40] 8. Adirondack-class rocks (olivine-rich basalts from the Gusev plains) represent a primitive magma composition [*Monders et al.*, 2006] formed by melting at $\sim$1.0 GPa and thus could be parental to fractionated magmas. Oxide components of Irvine, Backstay, and Wishstone generally fall on or near calculated liquid lines of descent for Adirondack-class basalt melt calculated using MELTS at pressures of $\sim$0.1 GPa (Irvine), $\sim$0.2 GPa (Backstay), and $\sim$1.0 GPa (Wishstone). Discrepancies for some elements occur, especially for the high-pressure model, that might reflect sorting of ash components in Wishstone.

[41] 9. These alkaline rocks are hypothesized to have formed by fractional crystallization at various depths of oxidized, hydrous basaltic magmas similar in composition to Adirondack-class rocks. If correct, they may be part of the same magmatic system that produced primitive picritic lavas on the Gusev plains. The fractionated magmas in the Hills may have been emplaced coevally with plains lavas (if the float represents dikes that intruded the Hills) or earlier (if the float represents ejecta lofted in from other locations but not present on the plains).

[42] 10. Regardless of their time of emplacement, the compositions of these rocks reveal the alkaline nature of the Gusev magmatic province. These rocks constitute the first definitive observation of alkaline rocks on Mars.

[43] 11. The alkaline affinities of all the Gusev volcanic rocks, as well as their limited patterns of distribution, may suggest a local magmatic source for Irvine-, Backstay-, Wishstone-, and Adirondack-class volcanic rocks under Gusev crater, rather than derivation from a more distant volcanic center.

References

Adams, J. B. (1974), Visible and near-infrared diffuse reflectance of pyroxenes as applied to remote sensing of solid objects in the solar system, *J. Geophys. Res.*, *79*, 4829–4836.

Arvidson, R. E., et al. (2006), Overview of the Spirit Mars Exploration Rover Mission to Gusev Crater: Landing site to Backstay Rock in the Columbia Hills, *J. Geophys. Res.*, *111*, E02S01, doi:10.1029/2005JE002499.

Ballhaus, C., and B. R. Frost (1994), The generation of oxidized CO_2-bearing basaltic melts from reduced CH_4-bearing upper mantle sources, *Geochim. Cosmochim. Acta*, *58*, 4931–4940.

Bandfield, J. L., V. E. Hamilton, and P. R. Christensen (2000), A global view of Martian surface compositions from MGS-TES, *Science*, *301*, 1084–1087.

Bell, J. F., III, W. H. Farrand, J. R. Johnson, and R. V. Morris (2002), Low abundance materials at the Mars Pathfinder landing site: An investigation using spectral mixture analysis and related techniques, *Icarus*, *158*, 56–71.

Bell, J. F., III, et al. (2003), Mars Exploration Rover Athena Panoramic Camera (Pancam) investigation, *J. Geophys. Res.*, *108*(E12), 8063, doi:10.1029/2003JE002070.

Bell, J. F., III, J. Joseph, J. N. Sohl-Dickstein, H. M. Arneson, M. J. Johnson, M. T. Lemmon, and D. Savransky (2006), In-flight calibration and performance of the Mars Exploration Rover Panoramic Camera (Pancam) instruments, *J. Geophys. Res.*, *111*, E02S03, doi:10.1029/2005JE002444.

Cabrol, N. A., E. A. Grin, R. Landheim, R. O. Kuzmin, and R. Greeley (1998), Duration of the Ma'adim Vallis/Gusev crater hydrogeologic system, Mars, *Icarus*, *133*, 98–108.

Christensen, P. R., et al. (2003), Miniature Thermal Emission Spectrometer for the Mars Exploration Rovers, *J. Geophys. Res.*, *108*(E12), 8064, doi:10.1029/2003JE002117.

Day, J. M. D., L. A. Taylor, C. Floss, and H. Y. McSween (2006), Petrology and chemistry of MIL 03346 and its significance in understanding the petrogenesis of nakhlites on Mars, *Meteorit. Planet. Sci.*, *41*, 581–606.

Dreibus, G., and H. Wänke (1985), Mars, a volatile-rich planet, *Meteoritics*, *20*, 367–381.

Dunn, T. L., and H. Y. McSween (2005), Identification of alkalic rocks using thermal emission spectroscopy: Applications to Martian remote sensing, *Meteorit. Planet. Sci.*, *40*, suppl., Abstract A42.

Farrand, W. H., J. F. Bell III, J. R. Johnson, S. W. Squyres, J. Soderblom, and D. W. Ming (2006), Spectral variability among rocks in visible and near-infrared multispectral Pancam data collected at Gusev crater: Examinations using spectral mixture analysis and related techniques, *J. Geophys. Res.*, *111*, E02S15, doi:10.1029/2005JE002495.

Foley, C. N., T. Economou, and R. N. Clayton (2003), Final chemical results from the Mars Pathfinder alpha proton X-ray spectrometer, *J. Geophys. Res.*, *108*(E12), 8096, doi:10.1029/2002JE002019.

Gellert, R., et al. (2004), Chemistry of rocks and soils in Gusev Crater from the Alpha Particle X-ray Spectrometer, *Science*, *305*, 829–832.

Gellert, R., et al. (2006), Alpha Particle X-Ray Spectrometer (APXS): Results from Gusev crater and calibration report, *J. Geophys. Res.*, *111*, E02S05, doi:10.1029/2005JE002555.

Ghiorso, M. S., and R. O. Sack (1995), Chemical mass transfer in magmatic processes, IV. A revised and internally consistent thermodynamic model for the interpolation and extrapolation of liquid-solid equilibria in magmatic systems at elevated temperatures and pressures, *Contrib. Mineral. Petrol.*, *119*, 197–212.

Hamilton, V. E., M. B. Wyatt, H. Y. McSween, and P. R. Christensen (2001), Analysis of terrestrial and Martian volcanic compositions using thermal emission spectroscopy, *J. Geophys. Res.*, *107*(E6), 14,733–14,746.

Herkenhoff, K. E., et al. (2003), Athena Microscopic Imager investigation, *J. Geophys. Res.*, *108*(E12), 8065, doi:10.1029/2003JE002076.

Herkenhoff, K. E., et al. (2006), Overview of the Microscopic Imager Investigation during Spirit's first 450 sols in Gusev crater, *J. Geophys. Res.*, *111*, E02S04, doi:10.1029/2005JE002574.

Hyndman, D. W. (1972), *Petrology of Igneous and Metamorphic Rocks*, 533 pp., McGraw-Hill, New York.

Irvine, T. N., and W. R. A. Baragar (1971), A guide to the chemical classification of the common volcanic rocks, *Can. J. Earth. Sci.*, *8*, 523–548.

Klingelhöfer, G., et al. (2003), Athena MIMOS II Mössbauer spectrometer investigation, *J. Geophys. Res.*, *108*(E12), 8067, doi:10.1029/2003JE002138.

Le Bas, M. J., R. W. Le Maitre, A. Streckeisen, and B. Zanettin (1986), A chemical classification of volcanic rocks based on the total alkali-silica diagram, *J. Petrol.*, *27*, 745–750.

Le Maitre, R. W. (2002), *Igneous Rocks: A Classification and Glossary of Terms*, Cambridge Univ. Press, New York.

Lodders, K., and B. Fegley Jr. (1997), An oxygen isotope model for the composition of Mars, *Icarus*, *126*, 373–394.

Martínez-Alonso, S., B. M. Jakosky, M. T. Mellon, and N. E. Putzig (2005), A volcanic interpretation of Gusev Crater surface materials from thermophysical, spectral, and morphological evidence, *J. Geophys. Res.*, *110*, E01003, doi:10.1029/2004JE002327.

McSween, H. Y. (2002), The rocks of Mars, from far and near, *Meteorit. Planet. Sci.*, *37*, 7–25.

McSween, H. Y., Jr., T. L. Grove, and M. B. Wyatt (2003), Constraints on the composition and petrogenesis of the Martian crust, *J. Geophys. Res.*, *108*(E12), 5135, doi:10.1029/2003JE002175.

McSween, H. Y., et al. (2004), Basaltic rocks analyzed by the Spirit rover in Gusev crater, *Science*, *305*, 842–845.

McSween, H. Y., et al. (2006), Characterization and petrologic interpretation of olivine-rich basalts at Gusev Crater, Mars, *J. Geophys. Res.*, *111*, E02S10, doi:10.1029/2005JE002477.

Ming, D. W., et al. (2006), Geochemical and mineralogical indicators for aqueous processes in the Columbia Hills of Gusev crater, Mars, *J. Geophys. Res.*, *111*, E02S12, doi:10.1029/2005JE002560.

Monders, A. G., E. Medard, and T. L. Grove (2006), Basaltic lavas at Gusev crater revisited, *Lunar Planet Sci.* [CD-ROM], *XXXVII*, Abstract 1834.

Morris, R. V., et al. (2004), Mineralogy at Gusev crater from the Mössbauer Spectrometer on the Spirit rover, *Science*, *305*, 833–836.

Morris, R. V., et al. (2006), Mössbauer mineralogy of rock, soil, and dust at Gusev crater, Mars: Spirit's journey through weakly altered olivine basalt on the plains and pervasively altered basalt in the Columbia Hills, *J. Geophys. Res.*, *111*, E02S13, doi:10.1029/2005JE002584.

Mustard, J. F., and J. M. Sunshine (1995), Seeing through the dust: Martian crustal heterogeneity and links to the SNC meteorites, *Science*, *267*, 1623–1626.

Mustard, J. F., S. Erard, J.-P. Bibring, J. W. Head, S. Hurtrez, Y. Langevin, C. M. Pieters, and C. J. Sotin (1993), The surface of Syrtis Major: Composition of the volcanic substrate and mixing with altered dust and soil, *J. Geophys. Res.*, *98*(E2), 3387–3400.

Nekvasil, H., A. Simon, and D. H. Lindsley (2000), Crystal fractionation and the evolution of intra-plate hy-normative igneous suites: Insights from their feldspars, *J. Petrol.*, *41*(12), 1743–1757.

Nekvasil, H., J. Filiberto, M. Whitaker, and D. H. Lindsley (2003), Magmas parental to the Chassigny meteorite: New considerations, in *Sixth International Conference on Mars* [CD-ROM], Abstract 3041, Lunar and Planet. Inst., Houston, Tex.

Nekvasil, H., A. Dondolini, J. Horn, J. Filiberto, H. Long, and D. H. Lindsley (2004), The origin and evolution of silica-saturated alkalic suites: An experimental study, *J. Petrol.*, *45*, 693–721.

Rieder, R., R. Gellert, J. Brückner, G. Klingelhöfer, G. Dreibus, A. Yen, and S. W. Squyres (2003), The new Athena alpha particle X-ray spectrometer for the Mars Exploration Rovers, *J. Geophys. Res.*, *108*(E12), 8066, doi:10.1029/2003JE002150.

Ruff, S. W., et al. (2006), The rocks of Gusev crater as viewed by the Mini-TES instrument, *J. Geophys. Res.*, doi:10.1029/2006JE002747, in press.

Sanloup, C., A. Jambon, and P. Gillet (1999), A simple chondritic model of Mars, *Earth Planet. Sci. Lett.*, *112*, 43–54.

Stockstill, K. R., H. Y. McSween, and R. J. Bodnar (2005), Melt inclusions in augite of the Nakhla Martian meteorite: Evidence for basaltic parental melt, *Meteorit. Planet. Sci.*, *40*, 377–396.

Stolz, A. J. (1985), The role of fractional crystallization in the evolution of the Nandewar volcano, northeastern New South Wales, Australia, *J. Petrol.*, *26*, 1002–1026.

Squyres, S. W., et al. (2006), Rocks of the Columbia Hills, *J. Geophys. Res.*, *111*, E02S11, doi:10.1029/2005JE002562.

Wänke, H., and G. Dreibus (1988), Chemical composition and accretion history of terrestrial planets, *Philos. Trans. R. Soc. London, Ser. A*, *325*, 545–557.

Wänke, H., J. Brückner, G. Dreibus, R. Rieder, and I. Ryabchikov (2001), Chemical composition of rocks and soils at the Pathfinder site, *Space Sci. Rev.*, *96*, 317–330.

————————

J. F. Bell III and S. W. Squyres, Department of Astronomy, Cornell University, Ithaca, Space Sciences Building, NY 14853, USA.

P. R. Christensen and S. W. Ruff, Department of Geological Sciences, Arizona State University, Tempe, AZ 85287, USA.

J. A. Crisp, Jet Propulsion Laboratory, California Institute of Technology, Pasadena, CA 91109, USA.

R. Gellert, Department of Physics, University of Guelph, Guelph, ON, Canada N1G 2W1.

K. Herkenhoff, Astrogeology Branch, U.S. Geological Survey, Flagstaff, AZ 86001, USA.

T. J. McCoy and M. Schmidt, Department of Mineral Sciences, Smithsonian Institution, Washington, DC, USA.

H. Y. McSween and L. L. Tornabene, Department of Earth and Planetary Sciences, University of Tennessee, 306 Geological Sciences Building, Knoxville, TN 37996, USA. (mcsween@utk.edu)

D. W. Mittlefehldt and R. V. Morris, NASA Johnson Space Center, Mail Code SN3, Houston, TX 77058, USA.

K. R. Stockstill, Hawaii Institute of Geophysics and Planetology, University of Hawaii at Manoa, 1680 East-West Road, POST 602B, Honolulu, HI 96822, USA.